LOW-TEMPERATURE ELASTIC ANOMALIES AND HEAT GENERATION OF DEUTERATED PALLADIUM

NUCLEAR REACTION IN SOLIDS

KEYWORDS: *deuterated palladium, elastic anomalies, heat generation*

HIROO NUMATA *Tokyo Institute of Technology*
Department of Metallurgical Engineering, 2-12-1, O-okayama, Meguro, Tokyo 152, Japan

MIKIO FUKUHARA *Toshiba Tungaloy, Technical Research Laboratory*
Kokusai-Shinkawasaki Building, 1-50, 2 Chome, Kitakase
Saiwai-ku, Kawasaki 211, Japan

Received April 28, 1995
Accepted for Publication August 15, 1996

Elastic parameters (the Young's, shear, and bulk moduli; the Lamé parameter; the Poisson ratio; and the Debye temperature) and shear damping anomalies accompanied by the generation of excess heat (not less than 6 W) were observed between 116 and 190 K in deuterated palladium, $PdD_{0.719}$, suggesting dynamic interactions among deuterons squeezed between tetrahedral and octahedral interstices in the palladium face-centered-cubic lattice.

INTRODUCTION

Since Fleischmann and Pons[1] and Jones et al.[2] reported the possibility of the nuclear fusion of deuterium induced by electrochemical means in palladium at ambient temperatures, much work on the reproducibility of nuclear fusion has been carried out. Two areas of focus are the experimental confirmation of cold nuclear fusion and the theoretical mechanism for the nuclear fusion reactions. Confirmation has been sought for neutron, gamma-ray, tritium, and excess enthalpy measurements.[3] Indeed, in the conventional electrochemical method, Takagi et al.[4] and Numata et al.[5] observed burstlike neutron emissions with a 2.45-MeV energy spectrum at ambient temperature during long-term electrolysis of palladium, which exhibited a more negative potential than that expected from the Tafel relation at a current density of 100 A/m^2. The sporadic nature of neutron emission and the anomaly of the electrode potential were attributed to crystal imperfections such as lattice defects and grain boundaries. For the nonelectrochemical method, Menlove et al.[6] observed burst and random neutron emissions from titanium, which was subjected to deuterium gas and, subsequently, to multiple liquid nitrogen temperature cycles at ~243 K.

However, many objections have been raised with regard to the reproducibility of the cold nuclear fusion experiment.[7-11] In situ electrochemical methods are not necessarily suitable techniques for studying the reproducibility of nuclear fusion. Good reproducibility can be obtained from physical measurements of solid-state deuterated palladium and/or titanium. No one has reported a relationship between the generation of heat and solid-state physical anomalies for deuterated palladium, as far as we know.

Our interest lies in determining all the elastic moduli (Young's, shear, and bulk moduli; Lamé parameter,[a] Poisson ratio; and Debye temperature) and both dilational and shear internal frictions as well as the Debye temperature of the deuterated palladium at low temperatures from the standpoint of solid-state physics as opposed to the electrochemical data reported so far. As far as we know, no previous research has been conducted on the low-temperature, simultaneous measurement of all the parameters for the deuterated palladium, using both longitudinal and transverse waves with the same frequency. It is well known that the elastic parameters and the dielectric constants are important parameters for the evaluation of the physical features of solids. Because the longitudinal wave interacts with electrons and the transverse one lacks such interactions, simultaneous measurement provides such useful information about structural changes, lattice in-

[a]Lamé constants in isotropic solids are generally defined by two elastic constants, C_{12} and C_{44}, in the 6×6 elastic constant matrix. Strictly speaking, because Lamé constants are a function of temperature, "Lamé parameter" is used in place of "Lamé constants" in this study.

stabilities, and electronic contributions for deuterated palladium. If the lattice of the deuterated palladium shrinks on cooling to a critical radius for the dynamic reactions of deuterons, as suggested by the study of Menlove et al.,[6] the lattice system may experience changes in elastic behavior. Attention is given to the generation of excess heat in terms of atomic confinement in interstices of the palladium face-centered-cubic (fcc) lattice.

EXPERIMENTAL METHODS

The cold wrought 99.95% pure polycrystalline palladium rod[b] with a grain size of ~65 μm was first machined in the long form, which is composed of a 7-mm-diam, 9-mm-long rod and a 12-mm-diam, 40-mm-long screw with 1.75-mm-pitch threads to avoid the loss of ultrasonic wave propagation between a specimen and a waveguide. The former is used as the specimen, and the latter is taken as the waveguide for longitudinal waves. The threads prevent the generation of spurious signals by mode conversion at the sides in one run.[12] The form is shown in the cryostat system in Fig. 1 and is described in more detail later. The specimen with the waveguide was annealed at 1073 K for 10.8 ks in a 1-Pa vacuum and then cooled at a rate of 0.1 K/s in argon at ambient pressure. We subjected the specimen to further pretreatments: acid treatment for 10.8 ks and anodization at a current density of 0.3 A/m^2. The specimen with the waveguide was treated as an electrode bar under the following conditions.

Electrolysis was performed galvanostatically. The current levels were varied during the experiment; the

[b]Obtained from Nilaco.

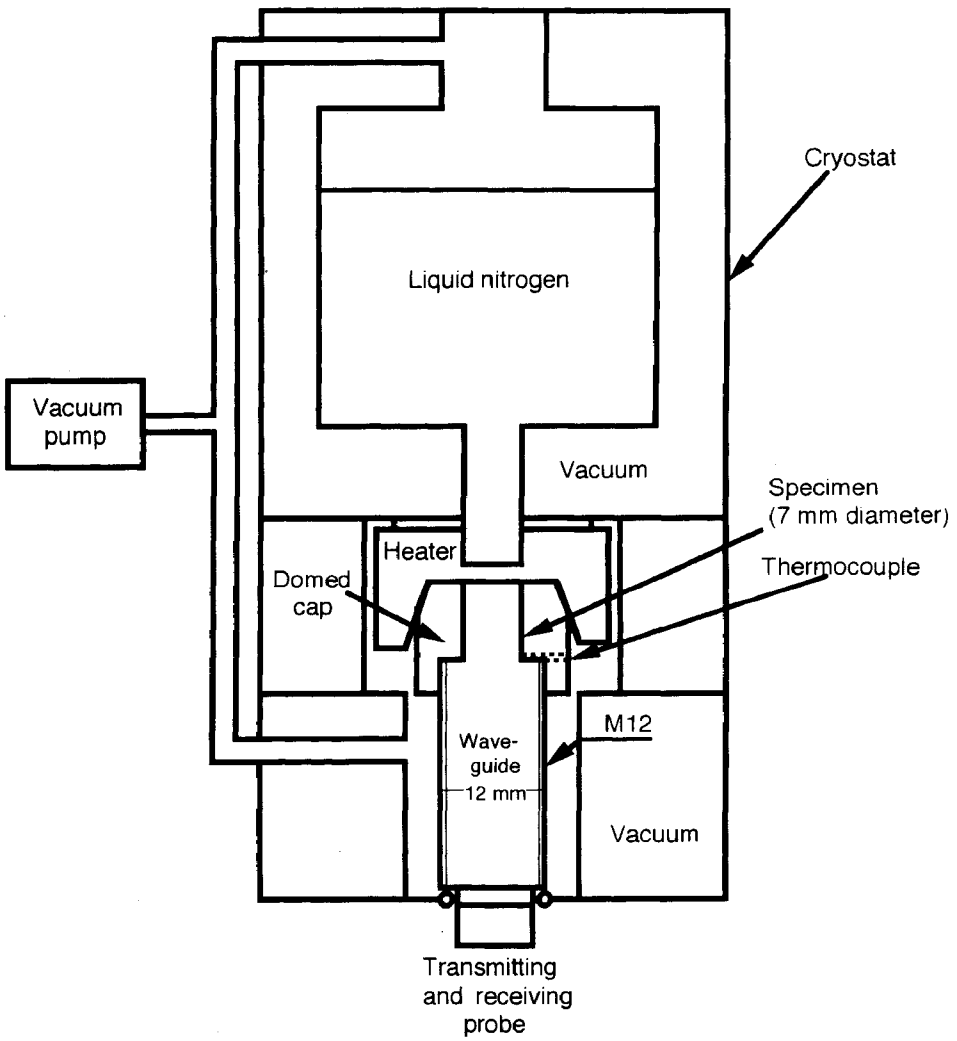

Fig. 1. Design of the cryostat system setting specimen. The long bar, which is composed of a 7-mm-diam, 9-mm-long specimen and a screw part (waveguide), is tightly inserted into the cryostat system.

direct-current density was raised step by step from 1 to 512 A/m^2 in ten steps with a holding time of 180 to 324 ks for each step.[4] An electrolyte of 0.1 *M* LiOD solution was prepared by the addition of 95% pure Li_2O[c] to 99.9% pure D_2O.[d] The electrochemical cell was a 170-ml Pyrex glass reaction vessel with a water jacket. The upper part of the cell was covered by a Teflon cap, from which were suspended working and counter electrodes and a thermistor. The palladium specimen cathode was placed in the center of the vessel and was suspended by a 0.5-mm-diam gold wire, which was welded to the bottom portion of the waveguide of the palladium electrode. A titanium anode, coated with a mixed oxide of platinum and iridium, was wound into a 42-mm-diam coil to fit snugly into the cell container tube.[e] The temperature of the circulating water was between 308 and 318 K. The molar volume of deuterium charged during electrolysis was estimated by in situ measurement[13] of the electrode potential and dilation of the specimen to obtain the β single phase.[14]

After electrolysis for 1 month, the electrochemical load caused axial flexing of ~1 mm from the centerline. After the gold wire was cut off the bottom of the waveguide, the specimen with the waveguide was straightened in a press to permit precise ultrasonic measurement. The density before and after charging was determined by the Archimedes method; the specimen was weighed both in air and in distilled water. Since we estimated that the evolution of deuterium from the palladium before density and ultrasonic measurements is not negligible, we measured the density of the charged specimen just before the ultrasonic measurement. The density was 7.1559 Mg/m^3, and the composition is estimated as $PdD_{0.719}$ by weighing, not by dilation. Longitudinal and transverse wave velocities and the corresponding values of attenuation were accurately measured with one longitudinal wave transducer at 30-s intervals using an ultrasonic pulse mode conversion method, based on zero cross-time detection.[15,16] To prevent oxidation of the deuterium and heat transfer problems caused by gas evolution, we kept the specimen at 1-Pa vacuum pressure. The design of the cryostat system holding the specimen is shown schematically in Fig. 1. A double-walled vessel was filled with liquid-nitrogen coolant. Cooling was promoted by lowering the pressure over liquid nitrogen down to 68 K. Heat from the specimen can propagate effectively through a copper-domed cap, which fastens the specimen to the waveguide. The present cryostat is the same as the one used in Refs. 17 through 20. The transducer and the waveguide were joined by water-free glycerin grease.[f] The joined portion was kept near room temperature, to avoid the low-temperature deterioration of piezoelectricity in PZT [$Pb(Zr_xTi_{1-x})O_3$] transducer material and solidification of the grease. A thermocouple, coated with alumina cement, was placed in a hole near the circumference of the specimen at the waveguide side.

To avoid propagation loss due to the high frequency of the ultrasonic wave, a longitudinal wave generation PZT transducer with a 4.9-MHz frequency was selected. Since a ratio of d (7.0 mm), the diameter of the specimen, to λ (1.16 mm), the wavelength, d/λ (6.1 at 298 K), is >2.5, the measured pulse velocity approaches the bulk velocity in an infinite elastic medium without interference between longitudinal and transverse waves.[17] In the ultrasonic pulse method, the shear modulus is a function of the transverse wave velocity only, while the Lamé parameter is a function of the velocities of both the longitudinal and the transverse waves. Thus, we can distinguish a physical meaning between pure mode III shear defined as shear modulus and three-dimensional mixed modes II and III shear described by the Lamé parameter. Internal friction in all the temperature region was calculated from the ratio of logarithm echo amplitude of the ultrasonic wave at given temperature to that at the lowest temperature.[16]

RESULTS

Generation of Excess Heat

The specimen was cooled at a rate of 0.1 K/s from room temperature. Experiment shows that our cryostat is capable of cooling from room temperature to 68 K within 1.8 ks. However, for the specimen used in this study, the cooling gradually became sluggish and then came to a standstill at 116 K (Fig. 2). Approximately 150 s after the

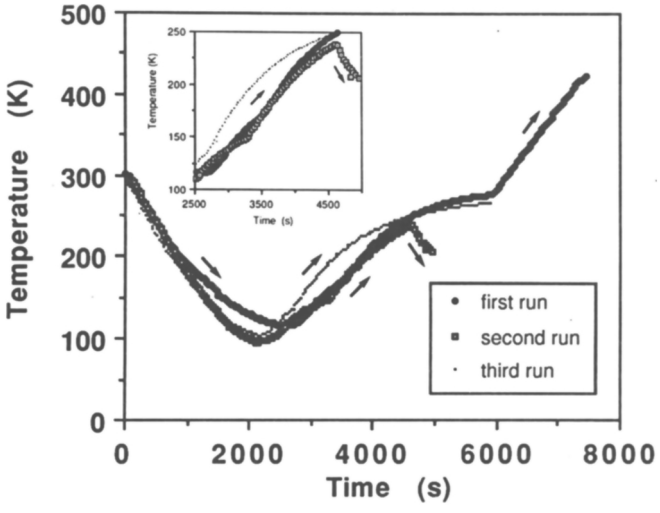

Fig. 2. Temperature of the sample as a function of time.

[c]Obtained from Wako Pure Chemicals.
[d]Obtained from Isotec.
[e]The Pt-Ir mixed coated titanium anode is currently used for industrial electrolysis, such as alkaline electrolysis and electroplating. This electrode has some advantages, such as good corrosion resistance, superior dimensional stability, etc.
[f]Obtained from Sonicoat SH.

standstill, the temperature began to increase at 0.064 K/s, rose up at 175 K, and finally saturated at 276 K. Then we heated the specimen at 0.1 K/s up to 423 K, which is the maximum temperature limit of the cryostat. After this experiment, we observed the remains of the liquid nitrogen in the cryostat. We are fully convinced that the increase in temperature is from the specimen.

The same experiment (the second run) was repeated after 5 days using the same specimen. The density of the specimen rose to 10.68 Mg/m^3 (estimated composition, $PdD_{0.198}$) due to evolution of the deuterium. The data of the second run are also illustrated in Fig. 2, showing a standstill at 96 K, then an increase up to 149 K, a saturation at 240 K, and a subsequent descent. Furthermore, 150 days after the first run, we observed similar behavior between 104 and 268 K in the third run without ultrasonic vibration, using a specimen with 10.81 density ($PdD_{0.179}$). However, we did not observe such increases in temperature for other materials in the low-temperature region, i.e., mild steel,[18] stainless steel,[18] (Y)TZP (yttria-stabilized tetragonal zirconia polycrystal),[19] fused quartz,[20] polymethyl methacrylate,[21] polyamide,[22] polycarbonate,[23] and polyvinyl chloride.[24]

Because the formation of β-PdDx ($x \geq 0.85$) due to absorption of deuterium is an exothermic process,[25] we cannot explain the rising-temperature phenomenon in the cooling run in a vacuum by the desorption of deuterium. The thermocouple was electrically shorted by coated alumina cement to the palladium specimen, so we can exclude the possibility of heat generation by thermoelectric effect. Thus, the abrupt increase in temperature from 116, 96, and 104 K in the first, second, and third runs, respectively, indicates the generation of excess heat from the specimen. To the best of our knowledge, however, no one has ever reported any phase transition accompanied by exothermic reaction in the low-temperature region between 96 and 116 K. The possibility that, given the imperfect vacuum, oxidation of either deuterium or lithium (remaining from the electrolysis) could account for the excess heat is evaluated in Appendixes A and B, where we show that the contributions are negligible. From the heat equilibrium calculation based on the heating data bank of this cryostat, the excess heat in the first run is estimated as 6 W or more (Appendix C).

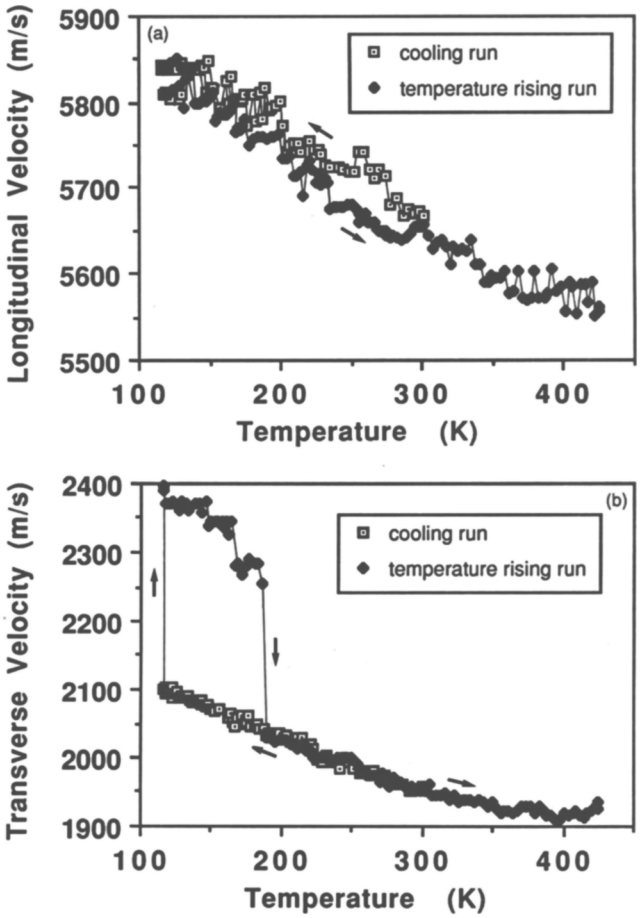

Fig. 3. Temperature dependence of (a) longitudinal and (b) transverse wave velocities for deuterated palladium.

Temperature Dependence of Elastic Moduli

The longitudinal and transverse wave velocities, V_l and V_t, respectively, as a function of temperature, are shown in Figs. 3a and 3b, respectively. Velocity V_l increases and decreases stepwise on almost the same curve between 209 and 116 K. This stepwise change suggests some reaction with longitudinal phonons in the strict sense of the word. On the other hand, V_t jumps suddenly by 14.2% at 116 K and decreases somewhat up to 190 K. Subsequently, it drops abruptly on the curve of the cooling run and then descends again as the temperature increases. The 116 K jump may be associated with the occurrence of excess heat. Both velocities of conventional solids increase monotonically with decreasing temperature, but we have occasionally observed discontinuity in V_l and V_t at temperatures at which phase changes occur. For the transverse velocity, a pronounced increase is associated with the change in morphology from a single crystal to a polycrystal of pure anthracene at 197 K (Ref. 26). For the longitudinal one, the order parameter is strongly connected with volume-nonpreserving distortions in a high-Tc superconductor at 117 K (Ref. 16).

Following previous papers,[15,16] the Young's, shear, and bulk moduli; the Lamé parameter; the Poisson ratio; and the Debye temperature in the first run alone were calculated from V_l and V_t. These results are presented in Figs. 4, 5, and 6, respectively. The temperature dependence curves of Young's and shear moduli are analogous to the transverse velocity curve. All elastic parameters increase substantially with decreasing temperature down to 116 K. In the spontaneous rising-temperature run, Young's and shear moduli jump suddenly by 28 and 30%

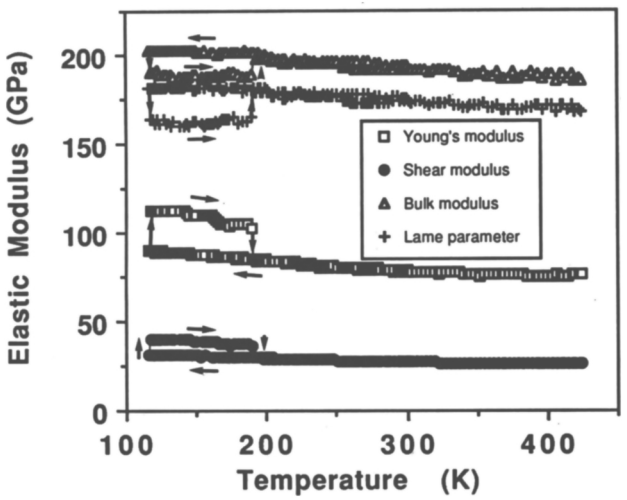

Fig. 4. Young's, shear, and bulk moduli and Lamé parameter of deuterated palladium as a function of temperature. Arrows show the direction of the change in temperature.

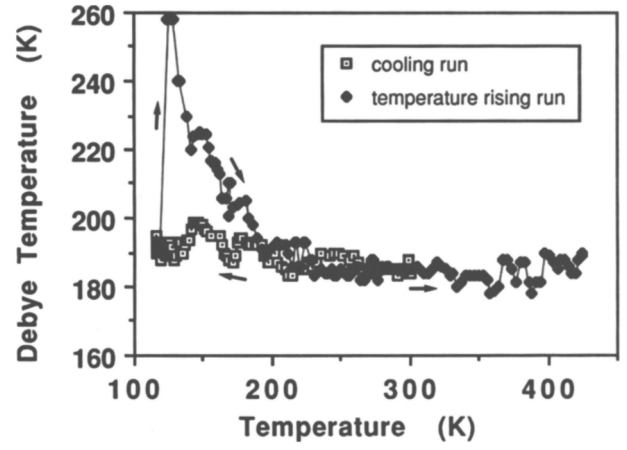

Fig. 5. Poisson ratio of deuterated palladium as a function of temperature. Arrows show the direction of the change in temperature.

at 116 K and drop abruptly by 18 and 19% at 190 K, respectively, on the cooling run curve and then descend again as temperature increases. This pronounced stiffening in the spontaneous rising-temperature run suggests that the atomic bonding strength of the lattice between 116 and 190 K is greater than that of the lattice between 190 and 425 K in the rising-temperature run and the lattice of the cooling run. By contrast, the bulk modulus and Lamé parameter represent opposite behaviors between 116 and 190 K in the spontaneous rising-temperature run; the former and the latter drop by 6 and 11% at 116 K and jump by 5 and 8% at 190 K, respectively, indicating a decrease in crystal rigidity between 116 and 190 K.

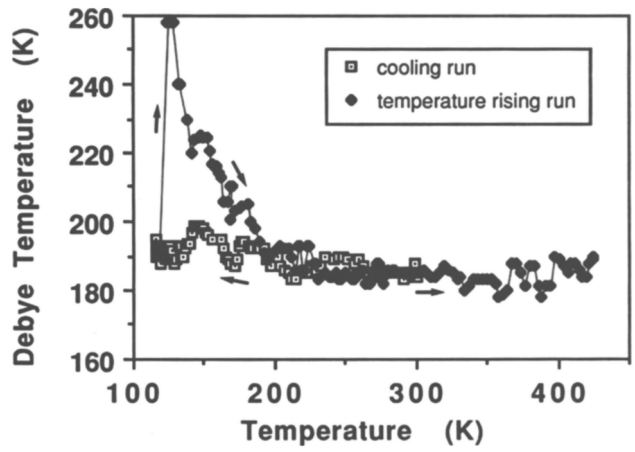

Fig. 6. Temperature dependence of the Debye temperature of deuterated palladium. Arrows show the direction of the change in temperature.

The temperature dependence of the Poisson ratio resembles that of the bulk modulus and the Lamé parameter in Fig. 4. However, since a decrease in the Poisson ratio means stiffness in the crystal lattice, this decrease between 116 and 190 K does not correspond physically to a decrease in the bulk modulus and the Lamé parameter but an increase in the Young and the shear moduli. Thus, the crystal lattice between 116 and 190 K is more rigid for simple (uniaxial) tension and shear, but it is more deformable for the three-dimensional mixed modes II and III shear described by the Lamé parameter and the three-dimensional volume-nonpreserving distortion defined as the bulk modulus.

In the elastic Debye temperature curve of Fig. 6, the Debye temperature jumps abruptly from 190 to 514 K at the end of the cooling run and then decreases parabolically down to 190 K during heat generation in the rising-temperature run. An increase in Debye temperature, i.e., an increase in the maximum frequency allowed, indicates a decrease in the effective ionic distance between movable deuterons in the palladium lattice.

In the second run, furthermore, we observed a similar elastic behavior in the lower temperature range between 96 and 118 K in the cooling and the rising-temperature runs: a continuous increase in the transverse wave velocity and the Young and the shear moduli, and a decrease in the bulk modulus, the Lamé parameter, and the Poisson ratio.

Temperature Dependence of the Internal Friction

Internal friction curves for longitudinal and transverse waves are shown as a function of temperature in Figs. 7a and 7b, respectively. The dilational friction in the rising-temperature run shows two small peaks at 200

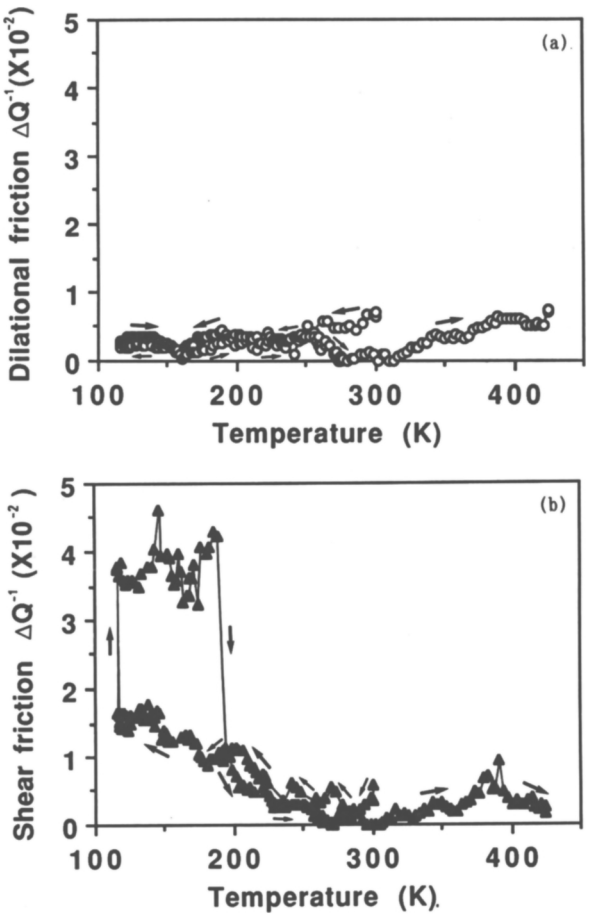

Fig. 7. Temperature dependence of internal friction for (a) longitudinal and (b) transverse waves of deuterated palladium. Arrows show the direction of the change in temperature.

and 250 K. Although these peaks seem to correspond to the 170 and the 225 K peaks in the cooling run, these peaks are not connected to uniaxial hardening between 116 and 190 K, where the elastic modulus anomalies were observed. Because there are so many possibilities regarding the origins of these peaks, e.g., mechanical damping by dislocation motion, migration of interstitial trapped deuterons,[27] etc., we cannot make any assignment at present. Further investigation is needed.

On the other hand, shear friction is more active than the dilational one: Shear friction shows a notable continuous damping behavior between 116 and 190 K in the rising-temperature run. This shear damping significantly correlates to a decrease in bulk modulus, Lamé parameter, and Poisson ratio, which are associated with a three-dimensional volume-nonpreserving distortion, not a uniaxial one.

In the second run, shear friction showed similar peaks at 113 and 120 K in the cooling and the rising-temperature runs, respectively.

DISCUSSION

Compared with the monotonic curve of transverse wave velocity in Fig. 3b, the longitudinal wave velocity curve shows stepwise progress in the temperature region between 209 and 116 K. Because the longitudinal waves result from the disturbance of the medium corresponding to a series of high- and low-pressure regions, the stepwise change may be associated with the alternating contraction and expansion of trapped interstitial deuterons in the palladium lattice. Another cause of this anomaly might be that the evolution of gas remaining from the palladium during the experiment may have caused poor contact between the transducer and the waveguide. However, the contact portion was kept near room temperature during the experiment, so we can eliminate this possibility. Even if the gas had evolved from the solid palladium, an adiabatic expansion arising from the solid-gas transition of deuterium occurs with a decrease in temperature in less than a microsecond.

There is a clear upper temperature of the anomaly in the ultrasonic data but not in the thermal data, as shown in Fig. 2. The two techniques agree about transition temperatures but disagree about the end time of the reaction. The ultrasonic technique seems to indicate the end point of the reaction. It is not clear, however, why the temperature increases for a long time up to saturation, even if heat is conducted from the interior source to the thermocouple for some time after the reaction ends.

If generation of the excess heat at 116 K correlates to dynamic interactions among deuterons in the palladium lattice, we must consider the crystallographic configuration of the deuteron of interest. In deuterated palladium PdD_x with $x > 0.75$ (Ref. 28), deuterium atoms occupy both the octahedral and tetrahedral interstices in the palladium fcc lattice: Six tetrahedral interstices form a cubic sublattice in the palladium fcc lattice, and one octahedral site lies at the center of the sublattice. A distance between tetrahedral-octahedral interstices along [111] directions is the shortest one, $\sqrt{3}a/4$, where a is a lattice parameter of palladium. Thus, there is a possibility that a dynamic interaction occurs among deuterons compressed from four tetrahedral sites along [111] directions to one central octahedral one. This compression requires an increase in crystal rigidity for simple (uniaxial) tension and shear. As can be seen from Fig. 4, the lattice between 119 and 190 K is stiffer for volume-nonpreserving motion such as alternating expansion and contraction.

Note that a breathing-mode displacement of the oxygen atoms in perovskite $BaBiO_3$ causes alternating expansion and contraction of the oxygen octahedra around the inequivalent Bi(I) and Bi(II) atoms[29] and leads to a complete charge disproportionation (charge-density wave instability) state, i.e., an alternating Bi^{3+}-Bi^{5+} array. Hence, by analogy, we suggest that a similar situation may occur for PdD_x.

As reported in previous studies of ceramics,[15,30] quartz,[31] metals,[32,33] and polymers,[21-24] the physical properties of the dilational friction are different from those of the shear one; a common characteristic of the former is the motion of dislocation along grain boundaries or the variation of potential energy between atoms, while that of the latter is atomic rearrangement in crystalline structure. Thus continuous damping in shear friction from 116 K would be perhaps related to atomic rearrangement among deuterons in the palladium lattice. However, the effects of an interstitial reaction on two elastic constants, C_{12} and C_{44}, are not clear. The effect of the reaction on these two C_{ij} will be discussed in a subsequent paper, using computer simulation.

In addition, because the longitudinal waves interact with conduction electrons, the lack of dilational damping between 116 and 190 K prevents an electric field.

CONCLUSION

Characteristic elastic and damping behaviors have been simultaneously measured as functions of temperature between 116 and 190 K in deuterated palladium, $PdD_{0.719}$. The temperature of the specimen is steady until midway (116 K) into the cooling run and then increases to 276 K. The Young and the shear moduli and the shear friction showed a continuous increase; the bulk modulus, the Lamé parameter, and the Poisson ratio revealed a corresponding decrease between 116 and 190 K in a spontaneous rising-temperature run. These results suggest the generation of excess heat associated with dynamic interactions among deuterons squeezed between tetrahedral and octahedral interstices in the palladium fcc lattice. The excess heat was estimated as 6 W or more. However, it is not clear whether the excess heat is derived from nuclear reactions or not. In subsequent papers, the neutron measurement and the hydrogen effect using palladium and titanium will be described.

APPENDIX A

POSSIBILITY OF OXIDATION OF DEUTERIUM

We estimate the heat of deuterium oxidation evolved from the palladium electrode during the measurement of the elastic properties in an imperfect vacuum. Since the molar quantity of palladium electrode material is calculated from the weight of the electrode, the gram-equivalent of palladium is

$$60.3\ \text{g}/106.4 = 0.567\ ,$$

where $M_{Pd} = 106.4$. Because the weight loss of deuterium evolved during the first rising-temperature run is estimated from the decrease in molar ratio of deuterium to palladium between the first and second runs, we obtain

$$0.567 \times (0.719 - 0.198) = 0.295\ \text{gram-equivalent}\ .$$

On the other hand, the heat of D_2O formation is

$$D_2 + \tfrac{1}{2}O_2 = D_2O\ ,$$
$$\Delta H_{298} = -294.6\ \text{kJ/mol (Ref. 34)}\ .$$

Consequently, the total amount of heat evolved during the rising-temperature run from 116 to 190 K for 3.97 ks is

$$(294.6/2) \times 1000 \times 0.295/3970 = 10.93\ \text{W}\ .$$

The amount of D_2O formation depends on the extent of O_2 donation, possibly due to vacuum leakage. Since the gas pressure in the specimen chamber was maintained at 1-Pa reduction pressure during the measurement, the total amount of real heat for D_2O formation is estimated, assuming idealistic gas behavior, to be

$$10.93 \times (1/101\,325) = 1.079 \times 10^{-4}\ \text{W}\ .$$

This estimated value is negligible compared with that experimentally obtained. Thus, the possibility that deuterium oxidation could be the cause of the excess heat can be distinctly eliminated.

APPENDIX B

POSSIBILITY OF OXIDATION OF LITHIUM

The heat of lithium oxidation in palladium can be evaluated in the same way as that of deuterium oxidation.

From an in-depth profile of the lithium concentration distribution in the lithium diffusion zone formed during heavy water electrolysis of palladium, the thickness of the lithium diffusion layer with an average concentration of 5 at.% lithium was estimated to be 1 μm (Ref. 35). Thus, we can roughly estimate the total amount of lithium that was deposited to the palladium electrode. Using the total surface area of specimen 2.8×10^3 mm^2, the total volume of the Pd-Li alloy layer is given by 2.8 mm^3. Since the density of the Pd–0.5 at.% Li alloy is 11.97×10^{-3} g/mm^3, we find that 3.352×10^{-2} g is the total weight of Pd-Li alloy layer. Using the 106.2 atomic weight of the Pd–0.5 at.% Li alloy and Avogardro number 6.02×10^{23}, the molar quantity of the Pd–0.5 at.% Li alloy layer was calculated as

$$3.352 \times 10^{-2}/106.2$$
$$= 3.156 \times 10^{-4}\ \text{gram-equivalent}\ .$$

From the 5 at.% lithium concentration, we obtain the total gram-equivalent of lithium:

$$3.156 \times 10^{-4} \times 0.05$$
$$= 1.578 \times 10^{-5}\ \text{gram-equivalent}\ .$$

The heat of lithium oxidation is

$$2\mathrm{Li} + \tfrac{1}{2}\mathrm{O_2} = \mathrm{Li_2O} \ ,$$
$$\Delta \mathrm{H}_{298} = -598.7 \text{ kJ/mol (Ref. 36)} \ .$$

Consequently, we obtain the total amount of heat evolved during the rising-temperature run from 116 to 190 K for 3.97 ks:

$$1.578 \times 10^{-5} \times 598.7 \times 1000 \times 0.5/3970$$
$$= 1.19 \times 10^{-3} \text{ W} \ .$$

This estimated value is still very small compared with that experimentally obtained. Thus, the possibility that lithium oxidation could be the cause of the excess heat can also be rigorously eliminated.

APPENDIX C

CALCULATION OF THE EXCESS HEAT

A cryogenic system must obey the conservation of energy law, so the algebraic sum of all forms of energy exchanged between the system and its surroundings must equal the resultant change in the energy of the system. Here, we limit ourselves to estimation of the heat from conduction because the kinetic and potential energy terms may usually be neglected in a closed-cycle refrigeration system. The accumulated heat content H transferred from the specimen and temperature controller can be expressed as the sum

$$H = -W_r + W_p + W_w + W_h + W_{ex} \ , \qquad \text{(A.1)}$$

where

W_r = refrigerating capacity due to liquid nitrogen

W_p = invasion heat transferred by the waveguide conduction

W_w = invasion heat transferred through the double-walled vacuumtight vessel

W_h = generation of heat by the heater

W_{ex} = generation of heat from an interior source.

On the other hand, H achieved by warmer temperature is expressed by the following relation:

$$H = \rho_{\mathrm{Cu}} \cdot V_{\mathrm{Cu}} \cdot Cp_{\mathrm{Cu}}(T) \cdot (dT/dt) + \rho_{p\mathrm{D}} \cdot V_{p\mathrm{D}} \cdot Cp_{p\mathrm{D}}(T) \cdot (dT/dt) \ , \qquad \text{(A.2)}$$

where

ρ_{Cu} = density of copper

$\rho_{p\mathrm{D}}$ = density of deuterated palladium

V_{Cu} = volume of copper domed cap

$V_{p\mathrm{D}}$ = volume of deuterated palladium

Cp_{Cu} = specific heat of copper at constant pressure

$Cp_{p\mathrm{D}}$ = specific heat of deuterated palladium at constant pressure

dT/dt = rate of warmup between 116 and 190 K.

Since we cannot obtain data for $Cp_{p\mathrm{D}}$, $Cp_{p\mathrm{H}}$ serves conveniently as a measure of calculation in place of $Cp_{p\mathrm{D}}$. We use the $Cp_{p\mathrm{H}}$ of hydrated palladium with the 0.5 H/Pd ratio, using an estimation formula, $n_{\mathrm{Pd}} \cdot Cp_{(\mathrm{Pd})} + n_{\mathrm{H}} \cdot Cp_{(\mathrm{H})}$ (Ref. 37), where $Cp_{(\mathrm{Pd})}$ and $Cp_{(\mathrm{H})}$ are the molar heat capacity of palladium and hydrogen, respectively, and n_{Pd} and n_{H} are the number of moles of palladium and hydrogen, respectively.

From Eqs. (A.1) and (A.2), we obtain W_{ex}:

$$W_{ex} = W_r - W_p - W_w - W_h + \rho_{\mathrm{Cu}} \cdot V_{\mathrm{Cu}} \cdot Cp_{\mathrm{Cu}}(T) \cdot (dT/dt) + \rho_{p\mathrm{D}} \cdot V_{p\mathrm{D}} \cdot Cp_{p\mathrm{D}}(T) \cdot (dT/dt) \ , \qquad \text{(A.3)}$$

where $W_r = 20$ W (from experimental data), and

$$W_p = \frac{A_p}{L_p} \int_T^{300} k_{p\mathrm{D}}(T)\, dT \ , \qquad \text{(A.4)}$$

$$W_w = z \cdot [I_{\mathrm{SS}}(300) - I_{\mathrm{SS}}(T)] \ , \qquad \text{(A.5)}$$

$$W_h = 0 \ , \qquad \text{(A.6)}$$

$$Cp_{\mathrm{Cu}}(T) = (-3.2103 \times 10^{-2} + 1.8516 \times 10^{-3} \cdot T + 2.1535 \times 10^{-5} \cdot T^2 - 1.0627 \times 10^{-7} \cdot T^3) \text{ (J/g·K) (Ref. 38)} \ , \qquad \text{(A.7)}$$

and

$$Cp_{p\mathrm{D}}(T) = (0.3459 - 7.9218 \times 10^{-3} \cdot T + 7.0197 \times 10^{-5} \cdot T^2 - 2.4876 \times 10^{-7} \cdot T^3 + 3.2579 \times 10^{-10} \cdot T^4) \text{ (J/g·K) (Ref. 39)}^{g} \ , \qquad \text{(A.8)}$$

where

L_p = length of the waveguide

A_p = cross-sectional area of the waveguide

z = distance between walls of the double-walled stainless steel (SS) vessel

I_{SS} = thermal conductivity integral of SS

$k_{p\mathrm{D}}$ = thermal conductivity of deuterated palladium.

[g] This equation was calculated by K. Ikeda, Taiyo-Toyo Sanso, Tokyo, Japan.

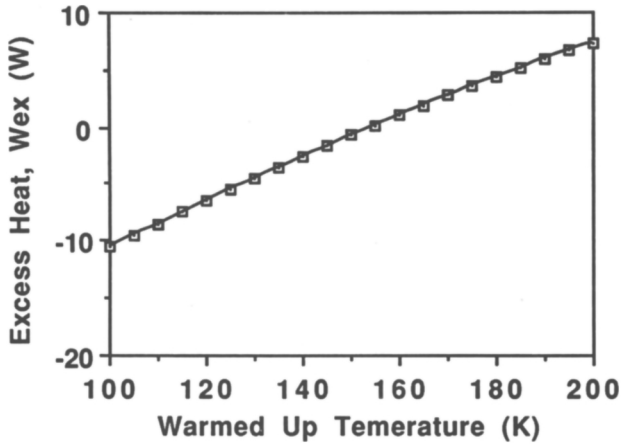

Fig. 8. The excess heat, W_{ex} as a function of the warmer temperature.

Since we cannot find $k_{pD}(T)$, we use the temperature-dependent thermal conductivity $k_{Pd}(T)$ of palladium for convenience. A comparison of $k_{Pd}(298)$ with $k_{PdH_{0.82}}(298)$ shows that the latter is 32% smaller than the former[40]:

$$I_{SS}(T) = (0.2021 + 1.1262 \times 10^{-2} \cdot T + 4.9082 \times 10^{-4} \cdot T^2 - 6.234 \times 10^{-7} \cdot T^3) \text{ (W/cm) (Ref. 41)} \quad \text{(A.9)}$$

and

$$k_{Pd}(T) = (1.6912 \times 10^4 - 1.4558 \times 10^4 \cdot \ln T + 5012 \cdot \ln T^2 - 859 \cdot \ln T^3 + 73.29 \cdot \ln T^4 - 2.49 \cdot \ln T^5) \text{ (W/m·K) (Ref. 42).} \quad \text{(A.10)}$$

Taking $\rho_{Cu} = 8.93$ kg/mm^3, $\rho_{pD} = 7.156$ kg/mm^3, $L_p = 40$ mm, $A_p = 92.68$ mm^2, $d = 0.112$ mm, $V_{Cu} = 2263$ mm^3, $V_{pD} = 396.335$ mm^3, $dT/dt = +0.06412$ K/s, we find W_{ex} as a function of the warmer temperature (Fig. 8). From Fig. 8, we get 6 W or more as the excess heat, taking into consideration the 32% smaller $k_{pD}(T)$.

ACKNOWLEDGMENTS

We would like to thank A. Sanpei, Toshiba Tungaloy, for help with ultrasonic measurement and K. Ikeda, Taiyo-Toyo Sanso, for aid with the calculation of excess heat.

REFERENCES

1. M. FLEISCHMANN and S. PONS, "Electrochemically Induced Nuclear Fusion of Deuterium," *J. Electroanal. Chem.*, **261**, 301 (1989).

2. S. E. JONES et al., "Observation of Cold Nuclear Fusion in Condensed Matter," *Nature*, **338**, 737 (Apr. 1989).

3. N. S. LEWIS et al., "Searches for Low-Temperature Nuclear Fusion of Deuterium in Palladium," *Nature*, **340**, 525 (1989).

4. R. TAKAGI, H. NUMATA, I. OHNO, K. KAWAMURA, and S. HARUYAMA, "Neutron Emission During a Long-Term Electrolysis of Heavy Water," *Fusion Technol.*, **19**, 2135 (1991).

5. H. NUMATA, R. TAKAGI, I. OHNO, K. KAWAMURA, and S. HARUYAMA, "Neutron Emission and Surface Observation During a Long-Term Evaluation of Deuterium on Pd in 0.1 M LiOD," *Proc. Conf. Science of Cold Fusion*, Vol. 33 of ACCF2, Como, Italy, June 29, 1991, p. 71, The Physics Society of Italy (1991).

6. H. O. MENLOVE, M. M. FOWLER, E. GARCIA, M. C. MILLER, M. A. PACIOTTI, R. R. RYAN, and S. E. JONES, "Measurements of Neutron Emission from Ti and Pd in Pressurized D_2 Gas and D_2O Electrolysis Cells," *J. Fusion Energy*, **9**, 495 (1990).

7. M. GAI et al., "Upper Limits on Neutron and γ-Ray Emission from Cold Fusion," *Nature*, **340**, 29 (1989).

8. D. E. WILLIAM et al., "Upper Bounds on 'Cold Fusion' in Electrolytic Cells," *Nature*, **342**, 375 (1989).

9. R. D. ARMSTRONG, E. A. CHARLES, I. FELLS, L. MOLYNEUX, and M. TODD, "Some Aspects of Thermal Energy Generation During the Electrolysis of D_2O Using a Palladium Cathode," *Electrochim. Acta*, **34**, 1318 (1989).

10. Z. SUN and D. TOMÁNEK, "Cold Fusion: How Close Can Deuterium Atoms Come Inside Palladium?" *Phys. Rev. Lett.*, **63**, 59 (1989).

11. S. E. JONES, D. E. JONES, D. S. SHELTON, and S. F. TAYLOR, "Search for Neutron, Gamma and X-Ray Emission from Pd/LiOD Electrolytic Cells: A Null Result," *Trans. Fusion Technol.*, **26**, 143 (1994).

12. A. SATHER, *J. Acoust. Soc. Am.*, **43**, 1291 (1960); see also H. J. McSKIMIN and E. S. FISHER, *J. Appl. Phys.*, **31**, 1627 (1960).

13. H. NUMATA, T. OOI, and I. OHNO, "In-Situ Potentio-Dilatometric Measurement of Hydrogen Absorption in Pd Electrode by Electrochemical Cathodic Loading Method," *Extended Abstracts Electrochemical Society Spring Mtg.*, Vol. 93-1, Hawaii, July 4, 1993, p. 2419, Electrochemical Society (1993).

14. E. WICKE, "Some Present and Future Aspects of Metal-Hydrogen Systems," *Z. Physik. Chem. Neue Folge*, **143**, S.1-21 (1985).

15. M. FUKUHARA and I. YAMAUCHI, "Temperature Dependence of the Elastic Moduli, Dilational and Shear Internal Frictions and Acoustic Wave Velocity for Alumina, (Y)TZP and β'-Sialon Ceramics," *J. Mater. Sci.*, **28**, 4681 (1993).

16. M. FUKUHARA and A. SANPEI, "Low-Temperature Elastic Moduli and Dilational and Shear Internal Frictions of Superconducting Ceramic $GdBa_2Cu_3O_{7-\delta}$," *Phys. Rev. B*, **49**, 13099 (1994).

17. L. Y. TU, J. N. BRENNAN, and J. A. SAUER, "Dispersion of Ultrasonic Pulse Velocity in Cylinder Rods," *J. Acoust. Soc. Am.*, **27**, 5505 (1955).

18. M. FUKUHARA and A. SANPEI, "Low Temperature-Elastic Moduli and Internal Dilational and Shear Friction of α-Iron and Stainless Steel" (unpublished).

19. M. FUKUHARA and A. SANPEI, "Low Temperature-Elastic Moduli and Internal Dilational and Shear Friction of (Y)TZP" (unpublished).

20. M. FUKUHARA and A. SANPEI, "Low Temperature-Elastic Moduli and Internal Dilational and Shear Friction of Fuzed Quartz," *J. Mater. Sci. Lett.* (in press).

21. M. FUKUHARA and A. SANPEI, "Low Temperature-Elastic Moduli and Internal Dilational and Shear Friction of Polymethyl Methacrylate," *J. Poly. Sci: Pt. B, Poly. Phys.*, **33**, 1847 (1995).

22. M. FUKUHARA and A. SANPEI, "Low Temperature-Elastic Moduli and Internal Dilational and Shear Friction of Polyimide," *J. Poly. Sci: Pt. B, Poly. Phys.*, **34**, 1579 (1996).

23. M. FUKUHARA and A. SANPEI, "Low Temperature-Elastic Moduli and Internal Dilational and Shear Friction of Polycarbonate," *Jpn. J. Appl. Phys.*, **35**, 3218 (1996).

24. M. FUKUHARA and A. SANPEI, "Low Temperature-Elastic Moduli and Internal Dilational and Shear Friction of Polyvinyl Chloride" (unpublished).

25. T. B. FLANAGAN, W. LUO, and J. D. CLEWLEY, "Calorimetric Enthalpies of Absorption and Desorption of Protium and Deuterium by Palladium," *J. Less-Common Met.*, **172–174**, 42 (1991).

26. A. MATSUI, M. FUKUHARA, and M. TAKEUCHI, "Temperature Dependence of Elastic Moduli, Internal Frictions and Debye Temperature for Anthracene Single Crystal" (unpublished).

27. K. HASHIMOTO and M. MESHII, "Measurements of Hydrogen Evolution from Pure Iron Between 77 and 800 K," *Scr. Metall.*, **19**, 1075 (1985).

28. B. BARANOWSKI, S. M. FILIPEK, M. SZUSTAKOWSKI, J. FARNY, and W. WORYNA, "Search for 'Cold-Fusion' in Some Me-D Systems at High Pressures of Gaseous Deuterium," *J. Less-Common Met.*, **158**, 347 (1990).

29. L. F. MATTHEISS and D. R. HAMMAN, "Electronic Structure of $BaPb_{1-x}Bi_xO_3$," *Phys. Rev. B*, **28**, 4227 (1983); see also S. UCHIDA, S. TAJIMA, A. MASAKI, S. SUGAI, K. KITAZAWA, and S. TANAKA, "Infrared Phonons in Superconducting Phase of $BaPb_{1-x}Bi_xO_3$," *J. Phys. Soc. Jpn.*, **54**, 4395 (1985).

30. M. FUKUHARA and Y. ABE, "High-Temperature Elastic Moduli and Internal Frictions of α-SiC Ceramic," *J. Mater. Sci. Lett.*, **12**, 681 (1993).

31. M. FUKUHARA and A. SANPEI, "High Temperature-Elastic Moduli and Internal Dilational and Shear Frictions of Fused Quartz," *Jpn. J. Appl. Phys.*, **33**, 2890 (1994).

32. M. FUKUHARA and A. SANPEI, "Elastic Moduli and Internal Friction of Low Carbon and Stainless Steels as a Function of Temperature," *Iron Steel Int.*, **33**, 508 (1993).

33. M. FUKUHARA and A. SANPEI, "Elastic Moduli and Internal Frictions of Inconel 718 and Ti-6Al-4V as a Function of Temperature," *J. Mater. Sci. Lett.*, **12**, 1122 (1993).

34. I. BARIN, *Thermodynamical Data of Pure Substances*, Part 1, p. 503, VCH Verlag, Weinheim, Germany (1989).

35. M. NAKADA, T. KUSUNOKI, M. OKAMOTO, and O. ODAWARA, "A Role of Lithium for the Neutron Emission in Heavy Water Electrolysis," *Proc. 3rd Int. Conf. Cold Fusion*, Nagoya, Japan, 1992, p. 581, H. IKEGAMI, Ed., Universal Academy Press, Tokyo (1993).

36. I. BARIN and O. KNACKE, *Thermodynamic Properties of Inorganic Substances*, p. 416, Springer Verlag, Dusseldorf, Germany (1973).

37. P. MITACEK, Jr., and J. G. ASTON, "The Thermodynamic Properties of Pure Palladium and Its Alloys with Hydrogen Between 30 and 300 K," *J. Am. Chem. Soc.*, **85**, 137 (1963).

38. T. SHIRAKI, A. HIRAI, and T. OKADA, *Handbook for Cryotechnology*, p. 581, Uchida Rokakuho, Tokyo (1982) (in Japanese); translated from *Lehrgangs Handbuch Kryotechnik*, Verein Deutscher Ingenieure, Arbeitskreis Kryotechnik der Deutschen Physikalischen Gesellschaft, Deutsch Arbeitsgemeinschaft Vakuum, Berlin (1977).

39. *Chronological Scientific Tables*, p. 466, National Astronomical Observatory, Maruzen, Tokyo (1987) (in Japanese).

40. A. W. SZAFRANSKI and B. BARANOWSKI, "Measurement of Heat Conductivity of Metals in an Environment of Compressed Gas, The Palladium/Hydrogen System up to 24 kbar at 25°C," *J. Phys. E*, **8**, 823 (1975).

41. T. SHIRAKI, A. HIRAI, and T. OKADA, *Handbook for Cryotechnology*, p. 583, Uchida Rokakuho, Tokyo (1982) (in Japanese).

42. *Chronological Scientific Tables*, p. 470, National Astronomical Observatory, Maruzen, Tokyo (1987) (in Japanese).

Hiroo Numata (D. Eng., materials engineering, Tokyo Institute of Technology, Japan, 1979) is a research associate at Tokyo Institute of Technology. His

current research activities are involved with the kinetic study of molten carbonate fuel cell electrode processors, electrodeposition from molten salts, and analysis of the metal hydrogen system.

Mikio Fukuhara (D. Eng., metallurgy, Osaka University, Japan, 1979) is a general manager at the Technical Research Laboratory at Toshiba Tungaloy. His current interests are material evaluations using ultrasonic measuring devices that he developed and the theory of superconductivity.